

## **XAFS and X-ray reflectivity study of III–V compound native oxide/GaAs interfaces**

**Seong-Kyun Cheong, Bruce A. Bunker, D. C. Hall, G. L. Snider and P. J. Barrios**

Copyright © International Union of Crystallography

Author(s) of this paper may load this reprint on their own web site provided that this cover page is retained. Republication of this article or its storage in electronic databases or the like is not permitted without prior permission in writing from the IUCr.

## XAFS and X-ray reflectivity study of III-V compound native oxide/GaAs interfaces

Seong-kyun Cheong,<sup>a</sup> Bruce A. Bunker,<sup>a</sup> D. C. Hall,<sup>b</sup> G. L. Snider,<sup>b</sup> P. J. Barrios<sup>b</sup>

<sup>a</sup>Department of Physics, University of Notre Dame, IN 46556, USA, <sup>b</sup>Department of Electrical Engineering, University of Notre Dame, IN 46556, USA. E-mail: bunker.1@nd.edu

Fluorescence-mode XAFS has been used to study the local environment about chosen atomic species such as Ga and As in bulk oxide  $\text{Al}_{1-x}\text{Ga}_x\text{As}$  ( $x=0.96$ ) and at the interface between thin (300 Å) oxidized  $\text{Al}_{1-x}\text{Ga}_x\text{As}$  ( $x=0.94$ ) film and GaAs substrate in total external-reflection mode. X-ray reflectivity experiments have also been employed to investigate the density profile of the oxide film on a GaAs substrate revealing the density profile as a function of depth. It is important to find out how the As is incorporated at the interface, the interfacial strain, and related local structural parameters for understanding that may be central in developing high performance III-V MOSFET devices.

**Keywords:** Reflection-mode XAFS; XANES; EXAFS; Reflectivity; Arsenic oxide; Gallium oxide; Gallium Arsenide

### 1. Introduction

New approaches for growing oxide films on AlGaAs using wet oxidation have been developed in the last several years (Dallesasse *et al.*, 1990; Chen *et al.*, 1995; DeMelo *et al.*, 2000). With a suitable gate oxide, AlGaAs/InGaAs/GaAs-based MOSFET devices could significantly outperform present Si electronics due to lower effective mass, higher electron mobility, and higher saturated velocity. In producing these insulating layers, however, the structure of the oxide and the nature of the interface are not well understood. The particular interest in this study is the role of residual As which is produced as a result of the oxidation. The As can produce Fermi-level pinning, increase leakage currents, and increase interface recombination. The goal of these studies is to correlate the physical structure to electronic properties and sample preparation methods.

The x-ray absorption fine-structure spectroscopy (XAFS) technique is near ideal for investigating the As and/or Ga environment. This technique is sensitive to the local structure about a chosen atomic species, revealing the types of nearby atoms and the radial distance distributions to these neighbors.

X-ray specular reflectivity was carried out to investigate the bulk properties such as the density profile as a function of depth, thickness of oxide layer and roughness of both surface and interface.

### 2. Materials and Methods

#### 2.1 As K-edge

A  $\sim 0.5 \mu\text{m}$   $\text{Al}_{0.96}\text{Ga}_{0.04}\text{As}$  film on a GaAs substrate was oxidized using techniques described previously (Ashby *et al.*, 1997). To study the As specifically in the oxide film and not in the substrate, the sample was mounted oxide-down to a glass slide using wax and the GaAs substrate was removed chemically with a phosphoric acid/hydrogen peroxide etch followed by a citric acid-hydrogen peroxide selective etch. For calibration standards used in the XAFS analysis, elemental As ( $\text{As}^0$ ), GaAs,  $\text{As}_2\text{O}_3$  ( $\text{As}^{3+}$ ), and  $\text{As}_2\text{O}_5$  ( $\text{As}^{5+}$ ) were obtained from standard chemical suppliers.

XAFS measurements were performed at the As K-edge at the Advanced Photon Source (APS) using the MRCAT undulator

beamline over the energy range 11,667–12,900 eV. XAFS data were obtained in transmission mode on standard samples to avoid distortions in XAFS for the concentrated samples and in fluorescence mode on the oxidized  $\text{Al}_{0.96}\text{Ga}_{0.04}\text{As}$  film.

#### 2.2 Ga K-edge

A thin 300 Å  $\text{Al}_{0.94}\text{Ga}_{0.06}\text{As}$  film on a GaAs substrate was surface-oxidized using the methods described as above. To investigate the density profile as a function of depth x-ray specular reflectivity was measured at the MRCAT ID-10 line using 8-circle Huber diffractometer. The x-ray energy was tuned at 300 eV above the Ga K-edge (10667 eV) and the dimension of the incident beam size was defined as approximately 50  $\mu\text{m}$  vertical width by 3 mm horizontal width. We employed two slits after the sample to reduce the background scattering and assure that all the beam reflected off the sample was detected – the slit dimensions were 400  $\mu\text{m} \times 5 \text{mm}$  for the first and 800  $\mu\text{m} \times 5 \text{mm}$  for the second slit.

Reflection-mode XAFS measurements were performed at the Ga K-edge over the energy range 10,167–11,100 eV in fluorescence mode and transmission-mode XAFS was measured for  $\text{Ga}_2\text{O}_3$  powder sample.

### 3. Results

#### 3.1 $\text{Al}_{0.96}\text{Ga}_{0.04}\text{As}$ oxide film

X-ray absorption near-edge structure (XANES) spectra for this work are largely used to “fingerprint” the As site. By comparing to other known As compounds, in favorable circumstances it is possible to match an unknown sample to a combination of known structures. We have made comparisons to elemental As, GaAs,  $\text{As}_2\text{O}_3$ , and  $\text{As}_2\text{O}_5$ . The absorption edge shifts to higher energy with increasing As oxidation state. The As K-edge XANES spectra of model compounds ( $\text{As}^0$ , GaAs,  $\text{As}^{3+}$  and  $\text{As}^{5+}$ ) and oxide sample are shown in Fig. 1(a). The x-ray energy origin was set at 11867 eV (K-edge of  $\text{As}^0$ ). As can be seen, none of these compounds singly agrees well with the oxide data. XANES spectrum of oxide shows that the sample contains primarily  $\text{As}^{3+}$ . It also has an additional feature at 10 eV indicating the presence of  $\text{As}^{5+}$  species. The spectrum is best fit by a combination of 80±10 %  $\text{As}_2\text{O}_3$  and 20±10 %  $\text{As}_2\text{O}_5$ ; the fit is shown in Fig. 1(b).

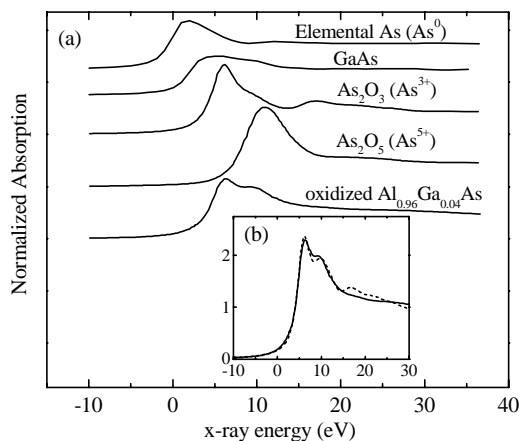


Figure 1. (a) XANES spectra of the oxide film (oxidized  $\text{Al}_{0.96}\text{Ga}_{0.04}\text{As}$ ) compared with analogous spectra for powders of elemental As, GaAs,  $\text{As}_2\text{O}_3$  and  $\text{As}_2\text{O}_5$ ; (b) XANES spectra of the oxide film (solid line) compared with a sum of 80 %  $\text{As}_2\text{O}_3$  and 20 %  $\text{As}_2\text{O}_5$  (dotted line).

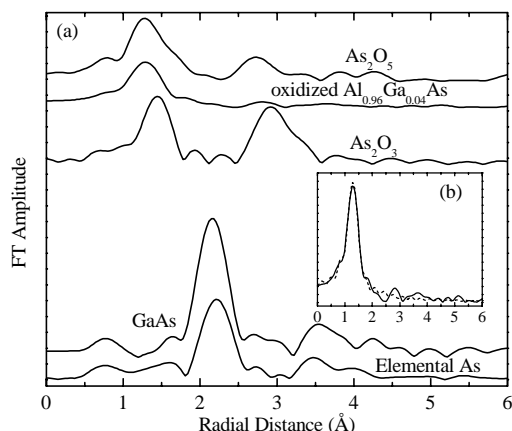


Figure 2. (a) Magnitudes of Fourier Transform (FT) of the As K-edge data for the oxide film (oxidized Al<sub>0.96</sub>Ga<sub>0.04</sub>As), elemental As, GaAs, As<sub>2</sub>O<sub>3</sub> and As<sub>2</sub>O<sub>5</sub>; (b) Magnitudes of Fourier Transform (FT) of the As K-edge oxide data (solid line) along with the simulation of 75 % As<sub>2</sub>O<sub>3</sub> and 25 % As<sub>2</sub>O<sub>5</sub> (dotted line). The Debye-Waller factors for the higher shells in the simulation are increased reflecting the disorder in the oxide sample

Fourier transforms of  $k^3\chi(k)$  were then compared to calculations from the multiple scattering computer code FEFF6.01 (Rehr *et al.*, 1992) and structural parameters were extracted using the program FEFFIT (Newville *et al.*, 1995). In the fits, the first four coordination shells were generally included in the analysis.

EXAFS spectra of the oxide sample were compared to those from model compounds – elemental As, GaAs, As<sub>2</sub>O<sub>3</sub>, and As<sub>2</sub>O<sub>5</sub> in Fig. 2(a), where As K-edge  $r$ -space data are shown. In this fitting, a number of structural models were considered, including interstitial or substitutional As in Al oxides or hydroxides, elemental As, GaAs, and the oxides As<sub>2</sub>O<sub>3</sub> and As<sub>2</sub>O<sub>5</sub>. None of these were consistent with the data.

However our XANES analysis suggests that ~80% of As<sup>3+</sup> and ~20% of As<sup>5+</sup> are present in the oxide sample. For independent EXAFS analysis theoretical EXAFS spectra are calculated using FEFF6.01 for As<sub>2</sub>O<sub>3</sub> and As<sub>2</sub>O<sub>5</sub> (Passegi *et al.*; As<sub>2</sub>O<sub>5</sub> has both tetrahedral and octahedral sites) and successfully fit to the measured As oxide samples with FEFFIT. Then we have fit the  $r$ -space EXAFS data of oxidized Al<sub>0.96</sub>Ga<sub>0.04</sub>As to those theoretical calculations of three first shells (one As<sub>2</sub>O<sub>3</sub> site and two As<sub>2</sub>O<sub>5</sub> sites). The best data fit, shown in Figure 2(b), is obtained by a combination of 75±20% As<sub>2</sub>O<sub>3</sub>, 21±20% As<sub>2</sub>O<sub>5</sub> tetrahedral site, and 4±20% As<sub>2</sub>O<sub>5</sub> octahedral site resulting large Debye-Waller factor (>0.01 Å<sup>2</sup>) for As<sub>2</sub>O<sub>3</sub> tetrahedral site when those two sites are decoupled, *i.e.* As<sub>2</sub>O<sub>5</sub> octahedral site contribution is negligible for EXAFS fit. This result is consistent with the independent XANES analysis of Figure 1 within uncertainty limits. Because of large disorder, the higher shell features of oxidized Al<sub>0.96</sub>Ga<sub>0.04</sub>As in Figure 2 are negligible comparing with the data of As<sub>2</sub>O<sub>3</sub> and As<sub>2</sub>O<sub>5</sub> suggesting that the residual As in Al<sub>0.96</sub>Ga<sub>0.04</sub>As converts to an amorphous matrix of As<sub>2</sub>O<sub>3</sub> and As<sub>2</sub>O<sub>5</sub> during the wet oxidation process.

### 3.2 Reflectivity (300 Å oxidized Al<sub>0.94</sub>Ga<sub>0.06</sub>As / GaAs)

For reflectivity analysis we used the model-independent methods (Sanyal *et al.*, 1996) based on the Distorted Wave Born Approximation (DWBA) (Sinha *et al.*, 1988). The general approach is as follows. We fixed the average electron density ( $\rho_0$ ), thickness ( $d$ ) of the film, and the roughness of surface ( $\sigma_1$ ) and interface ( $\sigma_2$ ) at the best value obtained by assuming a uniform density film. The film is then divided into a series of constant electron density slabs of

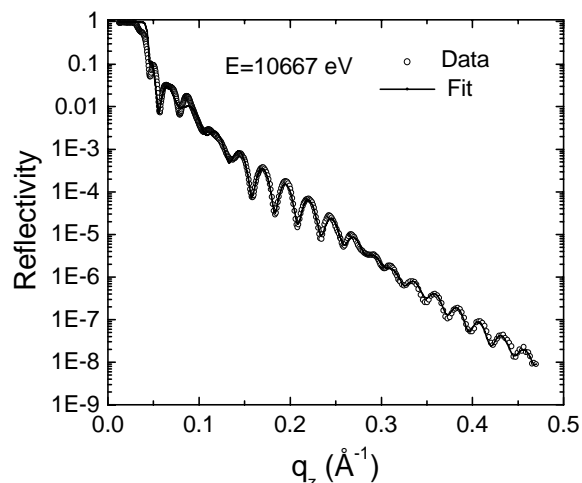


Figure 3 The measured x-ray reflectivity data of 300 Å oxidized Al<sub>0.94</sub>Ga<sub>0.06</sub>As / GaAs (open circles); best fit using a model-independent methods.

density  $\rho_0(z_i) + \Delta\rho(z_i)$ . Each slab has a width of  $\pi/q_{\max}$  where  $q_{\max}$  is the highest  $q_z$  reached by reflectivity scan. The values of  $\Delta\rho(z_i)$  in each slab are then varied until the best fit to the data is obtained. For this sample 33 slabs with 8 Å thickness each were used to describe a region up 264 Å deep from the surface.

The following are the best-fit values from the one-layer model (uniform density model):  $\rho_0 = 1.244 \text{ \AA}^{-3}$ ,  $d = 262.0 \pm 1.0 \text{ \AA}$ ,  $\sigma_1 = 5.3 \pm 0.5 \text{ \AA}$  and  $\sigma_2 = 5.0 \pm 0.5 \text{ \AA}$ . The resulting best fit from model-independent methods is shown in Figure 3 as a solid line through the data and the resulting density profile is shown in Figure 4.

A high electron density layer (~30 Å) exists at the surface with a density very close to that of GaAs, as can be seen in Figure 4, suggesting that the presence of a thin oxidized GaAs surface layer may be attributed to a residue of the original 500 Å GaAs protective cap not fully removed by a citric acid/hydrogen peroxide selective etch before oxidation. The presence of Ga at the surface was confirmed by both reflection-mode XAFS and X-ray photoelectron spectroscopy (XPS). A low-density layer (~60 Å) overlying higher

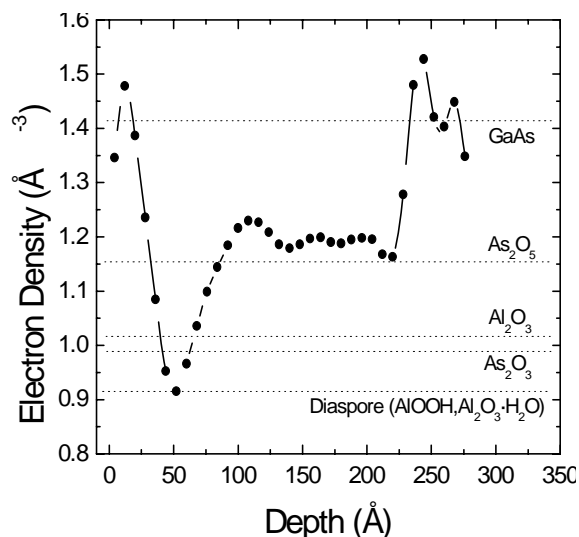


Figure 4 Calculated electron density profile from the model-independent fit (solid line with symbol); electron densities of several reference compounds (dashed lines)

density oxide layer (170 Å) is possibly due to the formation of lower density hydroxides than in the deeper layer.

### 3.3 Reflection-mode XAFS

Figure 5 shows a reflectivity scan for 300 Å oxidized  $\text{Al}_{0.94}\text{Ga}_{0.06}\text{As} / \text{GaAs}$  as a function of x-ray incident angle. The fluorescence data is obtained during a reflectivity scan at 300 eV above Ga edge (10667 eV). At an x-ray incident angle slightly

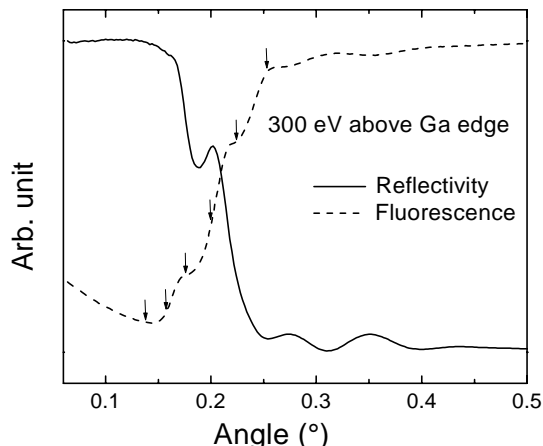


Figure 5. Reflectivity scan as a function of x-ray incident angle (solid line); Fluorescence data was taken during a reflectivity scan (dashed line); arrows indicate the angles XAFS were taken at

higher than the oxide critical angle, x-rays propagate through the top oxide layer (lighter layer) and totally reflect off the buried GaAs layer but can still penetrate a short distance into GaAs layer as an evanescent wave. As can be seen in Figure 5 the fluorescence intensity increases with angle, indicating the x rays are penetrating deeper into the GaAs. Eventually the x-ray incident angle reaches the critical value for GaAs, and the fluorescence signal gets saturated. XAFS measurements were taken at six different angles between 0.14° and 2.5°.

Figures 6 and 7 show that XANES and EXAFS respectively at each angle. GaAs feature is strong at the shallowest angle (0.14°) and the deepest angle (0.25°) in XANES and EXAFS both. In mediate angles XANES and EXAFS both show a mixture of Ga oxide and GaAs features and oxide feature is maximized at 0.175° in both cases. These reflection-mode XAFS scans at the Ga K-edge

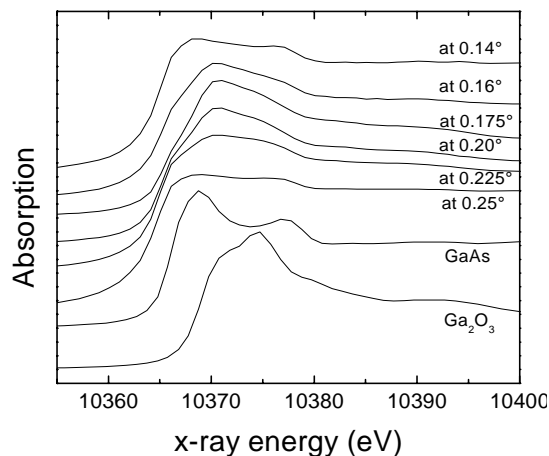


Figure 6 XANES spectra of 300 Å oxidized  $\text{Al}_{0.94}\text{Ga}_{0.06}\text{As} / \text{GaAs}$  at various x-ray incident angles and GaAs and  $\text{Ga}_2\text{O}_3$ .

are consistent with the electron density from the reflectivity fit.

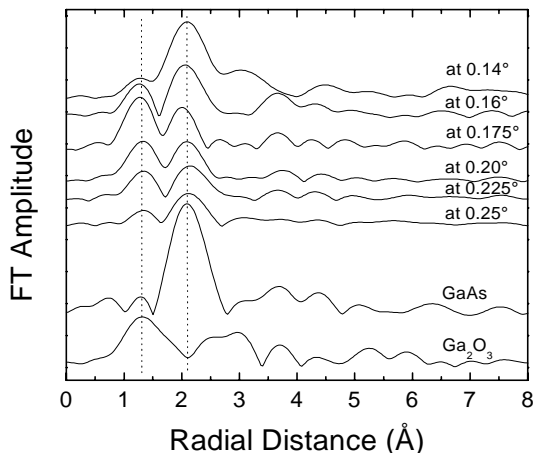


Figure 7. Magnitudes of Fourier Transform (FT) of the Ga K-edge data for 300 Å oxidized  $\text{Al}_{0.94}\text{Ga}_{0.06}\text{As} / \text{GaAs}$  at various x-ray incident angles, GaAs and  $\text{Ga}_2\text{O}_3$ .

### 4. Summary and Conclusions

Both EXAFS and XANES analyses of  $\text{Al}_{0.96}\text{Ga}_{0.04}\text{As}$  oxide film at As-edge show that the As in the wet-oxidized oxide appears to be a mixture of ~80 %  $\text{As}^{3+}$  and ~20 %  $\text{As}^5$  that are locally similar to  $\text{As}_2\text{O}_3$  and  $\text{As}_2\text{O}_5$ . To be consistent with our data, less than about 10% of the As atoms can be in elemental As, GaAs, or in interstitial or substitutional sites in Al oxides or Al hydroxides. Reflectivity and reflection-mode XAFS of oxidized  $\text{Al}_{0.94}\text{Ga}_{0.06}\text{As} / \text{GaAs}$  are consistent with each other and it is shown that these techniques can powerfully complement each other.

### References

Ashby, C. I. H., Sullivan, J. P., Newcomer, P. P., Missert, N. A., Hou, H. Q., Chen, E. I., Holonyak, Jr. N., and Maranowski, S. A. (1995). *Appl. Phys. Lett.* **66**(20), 2688-2690.  
 Dallesasse, J. M., Holonyak, Jr. N., Sugg, A.R., Richard, T. A., and Zein, N. El-. (1990). *Appl. Phys. Lett.* **57**(26), 2844-2846.  
 DeMelo, C. B., Hall, D. C., Snider, G. L., Xu, D., Kramer, G., and Zein, N. El-. (2000). *Electron. Lett.* **36**(1), 84-86.  
 Hammons, B. E., Hafich, M. J., and Baca A. G. (1997). *Appl. Phys. Lett.* **70**(18), 2443-2445.  
 Newville, M., Ravel, B., Haskel, D., Stern, E. A., Yacobi, Y. (1995). *Physica B* **208 & 209**(1-4), 154-156.  
 Passeggi, Jr. M.C.G., Vaquila, I., and Sferco, S.J. (1994) *Phys. Rev. B* **50**(4), 2090-2094.  
 Rehr, J. J., Albers, R. C., Zabinsky, S. I. (1992). *Phys. Rev. Lett.* **69**(23), 3397-3400.  
 Sanyal, M. K., Basu, J. K., Datta, A., and Banerjee, S. (1996). *Europhys. Lett.* **36**(4), 265-270.  
 Sinha, S. K., Sirota, E. B., Garoff, S., and Stanley, H. B. (1988). *Phys. Rev. B* **38**(4), 2297-2311.